Direct methods in photoelectron diffraction; experiences and lessons learnt based on the use of the projection method

2001 J. Phys.: Condens. Matter 13 10625

(http://iopscience.iop.org/0953-8984/13/47/307)

INSTITUTE OF PHYSICS PUBLISHING JOURNAL OF PHYSICS: CONDENSED MATTER

J. Phys.: Condens. Matter **13** (2001) 10625–10645 PII: S0953-8984(01)25745-2

Direct methods in photoelectron diffraction; experiences and lessons learnt based on the use of the projection method

D P Woodruff[1,3], P Baumgärtel[2], J T Hoeft[2], M Kittel[2] and M Polcik[2]

[1] Physics Department, University of Warwick, Coventry CV4 7AL, UK
[2] Fritz-Haber-Institut der Max-Planck-Gesellschaft, Faradayweg 4-6, 14195 Berlin, Germany

Received 13 June 2001
Published 9 November 2001
Online at stacks.iop.org/JPhysCM/13/10625

Abstract

As part of a programme of full quantitative adsorbate structure determinations on surfaces using scanned-energy-mode photoelectron diffraction (PhD) combined with multiple-scattering simulations, direct data-inversion methods based on Fourier transforms and the so-called projection method have been tested on experimental data from more than 30 adsorbate/substrate systems. The results highlight both strengths and weaknesses, many of which are likely to be generic in the use of direct methods. The most obvious feature is the reduced value of the methods for systems involving low emitter site symmetry or multiple-site occupation, but some specific problems attributed to the elastic scattering cross-section 'signatures' of different elemental species and cases in which multiple scattering proves to be especially important are also discussed. A combination of these problems in a particular system can lead to complete failure, although even in these cases the results are unlikely to be actively misleading as regards the correct structure.

1. Introduction

A very general problem of almost all methods of surface structure determination is that they rely on indirect 'trial-and-error' approaches, in which the experimental results are compared with the results of simulations based on a series of 'guessed' structural models until an acceptable fit is achieved. The methods of optimizing the fits and conducting more systematic and efficient searches of the structural parameter space have become quite sophisticated for some techniques, but the approach is intrinsically inefficient, and the ultimate solution is only as good as the imagination of the researchers conducting the data analysis: if the true structure is not included in the structural models tested, the solution will be incorrect, but not recognized as such. This fundamental problem has encouraged a succession of attempts over the years

[3] Also at: Fritz-Haber-Institut der Max-Planck-Gesellschaft, Faradayweg 4-6, 14195 Berlin, Germany.

to try to find approximate direct methods, akin to the use of Fourier transform methods and the associated Patterson functions in x-ray diffraction, which would render the analysis more efficient and more certain. These attempts have largely been directed to the techniques of low-energy electron diffraction (LEED) and photoelectron diffraction which share the same physical source of structural information through coherent interference of electrons elastically scattered by atoms in the surface.

As such, these methods are closely related to x-ray diffraction where direct methods have proved so successful in the past, but they have the same underlying complications that the low-energy scattering of electrons is very much stronger than that of x-rays, with the result that multiple scattering is very important, and that the scattering factors are intrinsically complex, introducing a phase shift in the scattering which depends on the electron energy, the scattering angle and the elemental character of the scatterer. All of these complications introduce phase differences between different scattered waves which, in a simple Fourier transform, are interpreted as changes in scattering path lengths, and thus as changes in atomic positions. Ultimately, the success of any method of directly inverting such data to give even an approximate idea of the real-space structure depends on the extent to which the influence of these complications can be suppressed or in some way taken into account. As a general statement, however, none of the methods presented so far take explicit account of all of these complications, but all rely on at least some of them not proving too important in a practical analysis. As such, they are all necessarily approximate methods. An approximate method undoubtedly has the potential to be extremely useful in a first-order analysis, but it is important not to lose sight of the fact that such a method can never replace proper multiple-scattering simulations in a final true structure determination.

In this paper we describe briefly the background to one direct method, the so-called projection method [1, 2], which was designed to provide first-order structural solutions from scanned-energy-mode photoelectron diffraction data, and try to draw together some general conclusions from our experience in applying this method to a large number of different experimental data sets. Attempting to understand problems experienced in a small number of systems has also led us to perform a limited number of model calculations aimed at trying to understand the origin of these problems more clearly. Although our conclusions are formally relevant only to the specific inversion method being used, many aspects of the different inversion methods proposed are similar, so there should be considerable commonality in the general problems encountered. This comment is important because most alternative methods of direct inversion have so far been applied to only a very small number of experimental data sets.

2. Scanned-energy-mode photoelectron diffraction and simple direct methods

During the last 10–15 years we have been involved in a major effort through a Warwick–Berlin collaboration to develop and apply the method of scanned-energy-mode photoelectron diffraction (PhD) to the determination of adsorbate structures (e.g. [3, 4]), and especially those involving molecular species on transition and noble metal surfaces, a group of problems broadly related to the general problem of gaining a fundamental understanding of aspects of heterogeneous catalysis. In this technique, the intensity of a core-level photoemission peak from an atom within an adsorbed species is measured in specific directions as a function of photon, and thus photoelectron, energy. The directly emitted component of the photoelectron wave-field interferes coherently with other components elastically scattered by surrounding (especially substrate) atoms, and as the photoelectron energy (and thus wavelength) is varied, these scattering paths switch in and out of phase, leading to modulations in the intensity. Adsorbates generally occupy sites above the substrate surface, so the experiments necessarily

involve backscattering, and are thus conducted at electron kinetic energies less than about 500 eV, for which backscattering cross-sections are reasonably large. In our approach truly quantitative structural solutions are obtained by fitting 5–10 such PhD modulation spectra, obtained in different emission directions, using multiple-scattering modelling and 'trial-and-error' identification of the best-fit structures (albeit aided by automated search and optimization routines). This approach has led to the solution of more that 50 substrate/adsorbate systems (e.g. [5]).

During this period of time there have been a number of attempts to demonstrate the potential of 'photoelectron holography', re-ignited most notably by Barton's paper of 1988 [6]. The initial objectives laid out in these papers, the great majority of which were based on simulated experimental data (using multiple-scattering calculations), was to obtain, through direct 'holographic reconstruction', an *approximate* but also reasonably unambiguous 'image' of the surroundings of the photoelectron emitter atoms, which would identify the emitter site and approximate bond length. Initially, at least, the goal was to achieve this inversion from a single-photoelectron-energy angular distribution (hologram), providing a direct analogue of a conventional single-wavelength hologram using visible light. While the original paper of Barton, inverting a simulated single-wavelength electron hologram for photoemission from S atoms in the well-known Ni(100)c(2 $\times$ 2)–S phase did lead to images which showed some features at positions known to correspond to those of near-neighbour Ni atoms, the quality was extremely low, with many spurious features and very poor resolution of the 'true' atomic images. Subsequently, a succession of theoretical studies suggested that using modified inversion algorithms, and starting with (simulated) holograms at several different photoelectron kinetic energies, more promising inversions of simple high-symmetry model structures appeared to be attainable. A very small number of experimental tests of these methods have been conducted, although many of these are on clean unreconstructed elemental solid surfaces rather than true surface phases.

While the methodology we had developed for structure determination by PhD was already proving very successful, there is no doubt that even very approximate structural information based on direct inversion of the experimental data could prove useful in the initial 'model guessing' stage of the structure determination, so we decided to explore some very simple ideas for direct inversion which followed the general spirit of the idea of holographic inversion but were not based on wide-angle scan 'holograms'. Our starting point in this was the recognition that we had found that a PhD modulation spectrum recorded in a direction which corresponds to 180° backscattering by a nearest-neighbour substrate atom typically shows strong modulations with a single dominant period (in electron wavevector) which corresponds to the path-length difference for this single-backscattering event. The reason for this appears to be partly related to the fact that atomic elastic scattering cross-sections commonly show a peak in this backscattering geometry (albeit very much weaker than that in the 0° forward-scattering geometry), although the high local symmetry of this geometry may also play a role. This suggests that these strong long-period modulations should be a 'signature' of the emitter–nearest-neighbour alignment direction, and if this direction can be found, the bonding site has been determined. Of course, because it is usually easy to make a good estimate of this nearest-neighbour bond length on the basis of the atoms involved, it is also possible to estimate the photoelectron energies at which this backscattering path should give maximal and minimal interference intensities, suggesting that angular scans at the appropriate energies might offer a route to directly establishing the backscattering direction directly.

This simple idea did show some promise [7], but it is far from clear how generally applicable it may be. Bearing in mind, however, that we were already routinely collecting scanned-energy-mode data (PhD spectra) in different emission directions, it seemed more

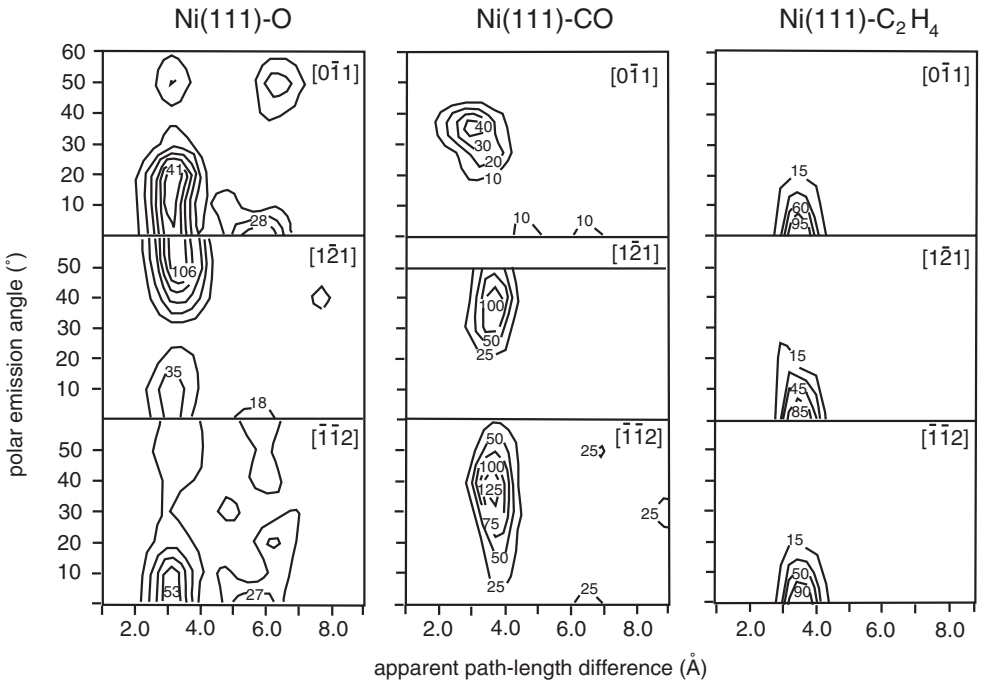

Figure 1. Fourier transform contour maps obtained from PhD data from O 1s emission in the Ni(111)/O system and C 1s emission from Ni(111)c(4 × 2)–CO and Ni(111)/C_2H_4. The maps are interpolated from PhD spectra taken at intervals of 10° in polar emission angle, in each of the three principle inequivalent azimuthal planes as defined in figure 2 (after [11]).

promising to try to use these data as the basis for a simple direct method. Our initial objective was to simply search through the PhD spectra for a specific adsorption system, trying to identify the one which most closely matched the criterion of having the largest-amplitude, long-period, dominant oscillation. The obvious way to identify this is to take Fourier transforms of each PhD spectrum (converted from photoelectron energy to photoelectron wavevector); the spectrum having a Fourier transform dominated by a large-amplitude single peak with an apparent path-length difference very approximately equal to twice the anticipated adsorbate–substrate bond length would be the one taken in a geometry most nearly aligned along the scatterer–emitter bond direction [8]. Notice that, even in the absence of multiple-scattering effects, the scattering phase shifts ensure that the apparent path-length difference does not exactly equal the actual path-length difference, but unlike some earlier attempts to use Fourier transforms of PhD spectra to determine the structure [9], our approach was not based on *apparent path lengths*, but on the *direction* of the PhD spectrum giving the largest-*magnitude* Fourier transform peak.

This method actually worked well on a number of model systems (e.g. [9, 10]). Figure 1 shows examples of the application of this method to PhD data from three different adsorbates on Ni(111), atomic O (O 1s emission from a (2 × 2) phase), CO (C 1s emission from the c(4 × 2) phase) and C_2H_4 (C 1s emission). In each case PhD spectra were collected at polar emission angles from normal emission (0°) to 60° in 10° steps in each of the three principal high-symmetry azimuths, [0$\bar{1}$1], [1$\bar{2}$1] and [$\bar{1}\bar{1}$2] (see figure 2). Each of these spectra was Fourier transformed and the moduli of the transforms from all spectra in a single azimuth were used, with simple interpolation, to plot a Fourier transform contour map using axes of polar

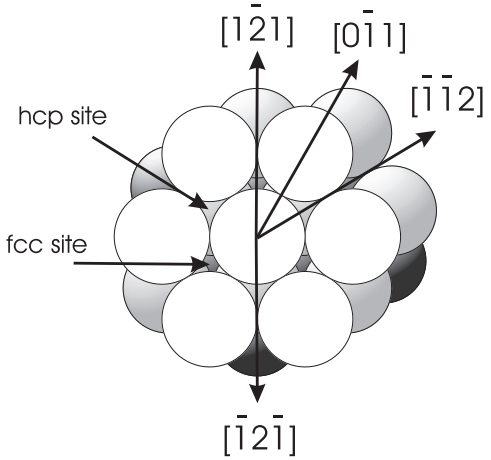

Figure 2. A plan view of an fcc(111) surface showing the definition of the azimuths used in figures 1 and 4 (below) and the two different hollow sites.

angle and apparent path-length difference. These are shown in figure 1. The amplitudes of the transforms have no absolute significance, but the scales used in the different azimuths for each species are comparable.

In the case of the data from the C_2H_4 adsorbate, the Fourier transforms all show a maximum intensity at an apparent path-length difference of approximately 3.6 Å and an emission angle of 0° (normal emission), clearly indicating that the C atoms occupy sites approximately atop surface Ni atoms; the true path-length difference in this case at normal emission would be twice the C–Ni bond length or about 3.9–4.0 Å. Notice that the C–C bond length in C_2H_4 in the gas phase is very much less than the Ni–Ni distance on the surface (2.49 Å), so if the molecule has its axis parallel to the surface (as is known to be the case) both C atoms cannot strictly occupy atop sites, but if the molecule adopts an aligned bridging site position (figure 3) the local C sites are off-atop. This issue of off-symmetry sites will become significant in our later discussion. Turning now to the data for chemisorbed O on Ni(111), the transforms show the largest peak at a somewhat similar apparent path-length difference (about 3.2 Å) in the $[1\bar{2}1]$ azimuth at a polar emission angle of about 50°. Comparison with the surface geometry seen in figure 2 shows that three Ni neighbours appear in this azimuth and its symmetry-equivalent azimuths if the O occupies a threefold-coordinated hollow site directly above a third-layer Ni atom—the so-called fcc hollow site. In this site (see also figure 3) the O atom will have O–Ni bonds tilted by an angle of around 50° to the surface normal. Finally the Fourier transforms for the C 1s PhD from CO adsorbed on this surface show essentially equivalent peaks in *both* the inequivalent ⟨211⟩ azimuths at polar angles of approximately 40°. This can be reconciled with equal occupation of the two inequivalent threefold-coordinated hollow sites (the fcc and hcp sites) on this fcc (111) surface. Full quantitative analysis confirmed these geometries [12, 13, 14].

3. The projection method

While this simple Fourier transform approach appears to be rather effective in identifying the adsorption site in a number of systems (it was used on about ten systems prior to being superseded by the projection method), it makes no attempt to determine the actual interatomic distances, and clearly requires that the experimental data set includes a PhD spectrum recorded

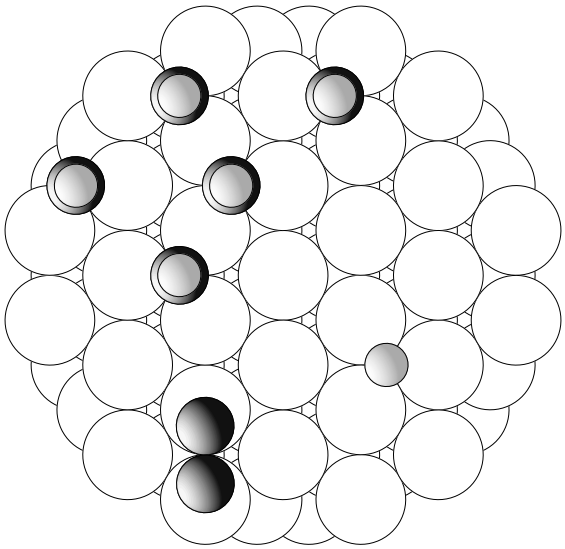

Figure 3. A plan view of a Ni(111) surface showing the C_2H_4, O and CO adsorption sites. The C atoms are shown most darkly shaded while the Ni atoms are shown unshaded. The radii of the O atoms has been arbitrarily reduced sufficiently for seeing the C atoms below in the adsorbed CO molecules. These are shown in the local ordering found in the c(4 × 2) phase.

in a direction very close to the emitter–near-neighbour bond direction. One potential route to overcoming these limitations was the 'projection method' of Hofmann and Schindler [1, 2]. A key underlying idea is that the major problem with using a Fourier transform to determine actual scattering path-length differences is that it takes no account of the phase shifts introduced in the dominant single-backscattering events which determine the main contribution to PhD spectra in a near-backscattering geometry. Of course, it is also true that multiple-scattering events introduce further phase factors, but these are neglected in essentially all direct inversion methods. At the very least, this must lead to inaccuracies in interatomic distances determined by these methods.

A standard Fourier transform has the form

$$u(\theta, \phi, r) = \int \chi_{ex}(\theta, \phi, k) \mathrm{e}^{\mathrm{i}kr} \, \mathrm{d}k$$

where $\chi_{ex}(\theta, \phi, k)$ is the experimental modulation function, dependent on the polar and azimuthal angles, θ and ϕ, and the photoelectron wavevector, k, and r defines a radial distance. In effect, therefore, the Fourier transform calculates the projection of the experimental modulation function onto a complex pure harmonic function with the periodicity in k defined by the real-space parameter r. In the absence of scattering phase shifts, the experimental single-scattering modulation spectrum would reflect this pure harmonic form. In the projection method we calculate instead, for a single experimental modulation function, the integral

$$c(\boldsymbol{r}) = \int \chi_{ex}(k) \chi_{th}(k, \boldsymbol{r}) \, \mathrm{d}k$$

where $\chi_{th}(k, \boldsymbol{r})$ is a theoretical single-scattering PhD modulation spectrum for a scattering atom placed at the location defined by the vector $\boldsymbol{r}$. Insofar as the experimental spectrum is dominated by a single-scattering event, this theoretical spectrum will have the same periodicity and phase as the experimental one (or the dominant component thereof) when $\boldsymbol{r}$ corresponds to

the true position of this dominant single-scattering atom. Computing this projection requires that one calculates the single-scattering spectrum expected at each possible position on some three-dimensional grid of points, but each of these calculations is essentially trivial yet does include the proper scattering phase shifts for the elemental species expected to be a near-neighbour backscatterer. Of course, this integral is based only on a single experimental modulation curve in a single direction, whereas the starting idea for the procedure (based on the Fourier transform method) is that the dominant single-scattering event will occur when the spectrum is recorded in the near-180° backscattering direction. One must therefore combine a series of $c_i(\boldsymbol{r})$ calculated for a range of i different spectra recorded in different emission directions in such a way as to ensure that the largest projection integrals dominate the final 'image'. The choice proposed for this combining function is

$$C(\boldsymbol{r}) = \sum_i \exp(Sc_i\boldsymbol{r})$$

with the exponential loading ensuring that only one or two integrals dominate, corresponding to those closest to the backscattering directions. The factor S (which is commonly set to unity) is an arbitrary scaling factor which can be used to modify the contrast of the 'image' defined by $C(\boldsymbol{r})$.

Figure 4 shows the result of applying this procedure to the same experimental data as were used in the Fourier transform method demonstration of figure 1. In this case we wish to display the results for the three-dimensional function, $C(\boldsymbol{r})$, which is done by showing two-dimensional sections in which the darkness of the half-tone 'image' is determined by the amplitude of $C(\boldsymbol{r})$. The upper panels show cuts perpendicular to the surface with the emitter (at (0, 0, 0)) just off the top of the panels. In each case dark streaks corresponding to scatterer positions are seen below the emitter, and the lower panels show cuts parallel to the surface at a depth chosen to pass through the maxima in C. What is clear from these 'images' is that the strong backscatterers appear as 'saucers'; the shape corresponds roughly to contours of constant effective scattering path length. Clearly the locations of these features correspond rather closely to the true Ni nearest-neighbour positions (figure 3) of the emitting adsorbate atoms.

4. Experimental applications of the projection method: a survey

Pursuing the original objective of a direct method in photoelectron diffraction, we have integrated the projection method into our standard methodology for structure determination [3, 4]. The projection method is first used to obtain an approximate local emitter geometry, and then the structure is refined using the full multiple-scattering simulations. Of course, the method is only intended to be approximate, so one must not lean too heavily on the approximate solution in excluding possible models. Typically, some limited tests of plausible geometries not obviously compatible with the projection method image are run to provide additional checks. There have also been a few cases in which the results of the method have proved too unspecific, or even occasionally, incompatible with any plausible structure on the known substrate. In most of these cases these problems are not unexpected. We first summarize some of the main findings before addressing some of the specific problems in more detail. The 30 or so systems studied can be most readily summarized according to the local adsorption geometry. Note that in all of these systems a full multiple-scattering analysis has been used to establish the full structure.

- *Face-centred cubic hollow sites on fcc(111) surfaces.* Structures falling into this group include Cu(111)/CH_3O–[10, 15], Cu(111)/Fe [16], Ni(111)/O [17], Ni(111)/CH_3O–[17], Ni(111)/Fe [18] and Pd(111)/CO [19]. All of these systems yielded reliable results.

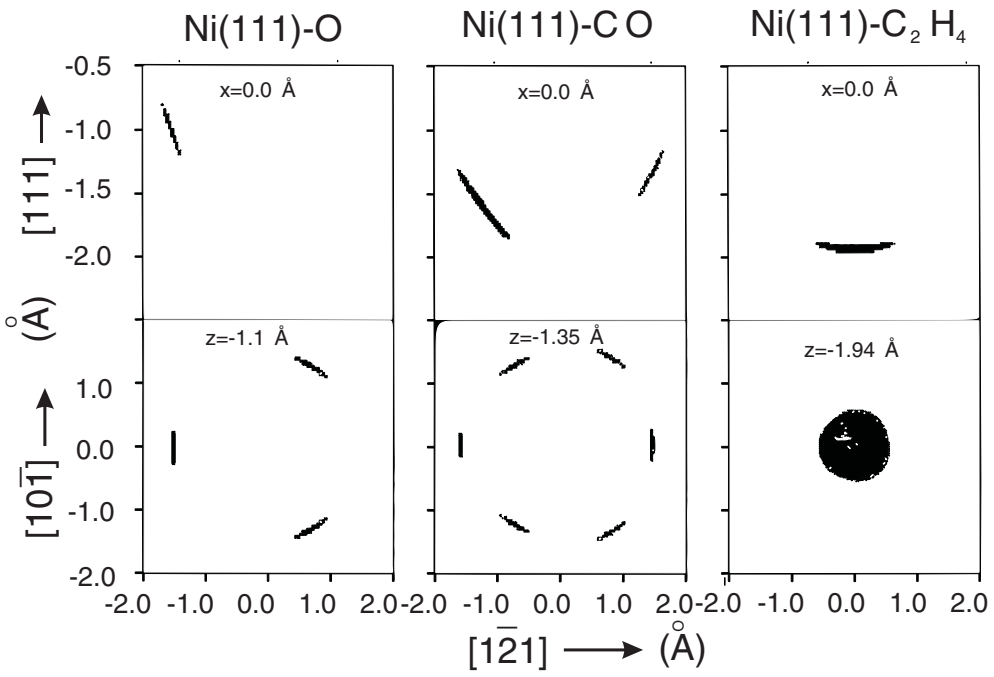

Figure 4. Projection method results from the same data used in figure 1. Greyscale 'images' are shown as cuts perpendicular to the surface (with the photoelectron emitter atom at $(0, 0, 0)$) and parallel to the surface at depths chosen to cut the main peaks seen in the perpendicular cuts. The darkest regions correspond to those most likely to be the position of a near-neighbour substrate atom (after [11]).

This is actually rather significant in the case of the Pd substrate because there appears to be a special potential problem with Pd scattering which did not show itself in the particular phase [20] appearing in this group; this is discussed in the following section.

- *Mixed fcc and hcp hollow site occupation on fcc(111) surfaces*. In this group we have Cu(111)/C_2H_2 [10], Cu(111)/$HCCCH_3$ and Cu(111)/$HCCCF_3$ [21], Ni(111)/C_2H_2 [22, 12], Ni(111)/CO [11, 14] and Ni(111)/NO [23]. In all of these systems the two hollow sites appear to be equally occupied (in the case of acetylene and the acetylenic C atoms in propyne, occupation of the two hollows is by the two C atoms in the same molecule). Not listed here are some CO and NO coadsorption systems that we have studied in which there may be only partial occupation of one site. In these systems, in particular, the direct method may only show one of the two sites. This is presumably partly dependent on the contrast factor S used in the imaging, and on the exact directions of the PhD spectra included in the experimental data set. Any imbalance in off-normal-emission spectra in the two inequivalent $\langle 211 \rangle$ azimuths (see figure 2) will clearly tend to favour one geometry when both sites are occupied. Notice too that the fact that two inequivalent sites are occupied inevitably means that the PhD modulations seen in any particular geometry are weaker, while the method is based on the idea that there are clear dominant spectral modulations in some directions. Bearing this in mind, these systems work well, but a clear moral is that one should not rely on the site shown by the projection method being the *only* site occupied. The case of the Pd(111)/CO phase in which both

sites are occupied equally failed to yield meaningful projection images, and is discussed in the following section.

- *Hollow sites on fcc(100) surfaces*. We have actually investigated rather few systems in this class. The substitutional adsorption of Mn on Cu(100) [24] appeared to work well, as did the Ni(100)/C [25] system at both low and high coverages, and the Cu(100)/O [26] system at low coverage. In the case of the higher-coverage (0.5 ML) Ni(100)/C system, the adsorbate induces a 'clock' reconstruction of the Ni surface inducing lateral movements of the outermost Ni layer atoms so as to produce 'zigzag' rows along the close-packed ⟨110⟩ azimuth. This symmetry lowering was not seen in the projection image, but as the data used in the inversion were only collected in the two high-symmetry azimuths of the substrate, this is not particularly surprising. We have, however, experienced a failure of the method in the case of the high-coverage (0.5 ML) Cu(100)/O and Cu(100)/N systems which will be discussed further below.
- *A hollow site on an fcc(110) surface*. Only one case, Cu(110)/Fe[27], has been investigated and this proved successful.
- *Bridge sites*. Only one case of bridge site adsorption has been investigated, that of Cu(110)/NH_x [28], and this was successful.
- *Atop sites*. While atop sites appear to be readily identified by direct methods, a rather general problem which we have identified is that in this adsorption geometry the vibrational amplitude parallel to the surface (the frustrated translational mode) is commonly of rather high amplitude. This has the effect of strongly damping (via a Debye–Waller type of factor) the coherent scattering for scattering paths with a significant component parallel to the surface. The net effect is that one typically sees strong PhD modulations in normal emission (the near-neighbour backscattering direction) but very weak modulations in all directions far removed from normal emission. Although a projection method inversion based on a data set centred around a small range of emission angles will lead to the atop site being properly identified, we have tended to take the view that this is something of a self-fulfilling prophesy, and have not generally used the projection method in these cases. A few cases in this category in which we have applied the method include Cu(110)/CO [29], Ni(111)CO/O (at room temperature) [30] and Cu(111)/NH_3 [31]. This last system actually yielded a projection 'image' which implied that the molecule is slightly off-atop, but it is difficult to determine from the full multiple-scattering analysis whether the adsorption is, or is not, exactly atop because one cannot readily distinguish the influence of a small static offset (averaged over several symmetry-equivalent directions) and a dynamic vibration of a similar amplitude.
- *Off-atop and other low-symmetry sites*. Low-symmetry adsorption sites in photoelectron diffraction can arise for two rather different reasons. In a small number of instances, an adsorbate may adopt a low-symmetry adsorption site, perhaps due to adsorbate-adsorbate interactions, a steric effect or a directional bond which is not along the surface normal. One such example is the case of NH_3 adsorption on Cu(110) [32]; the multiple-scattering analysis for this system showed a clear preference for a substantial static offset in addition to any dynamical vibration which was also seen in the projection image. Similar situations arose in the off-atop bonding of pyridine [33] and methyl pyridine [34] through the N atom on Cu(110). A further example is Si(100)/OH, but in this case only the Fourier transform method was used on a data set of restricted angular range [35].

A more common reason for low-symmetry emitter sites, however, is that in the case of molecular adsorption, intramolecular distances do not generally match substrate interatomic distances, so if intramolecular bonds have a component parallel to the surface, at least some

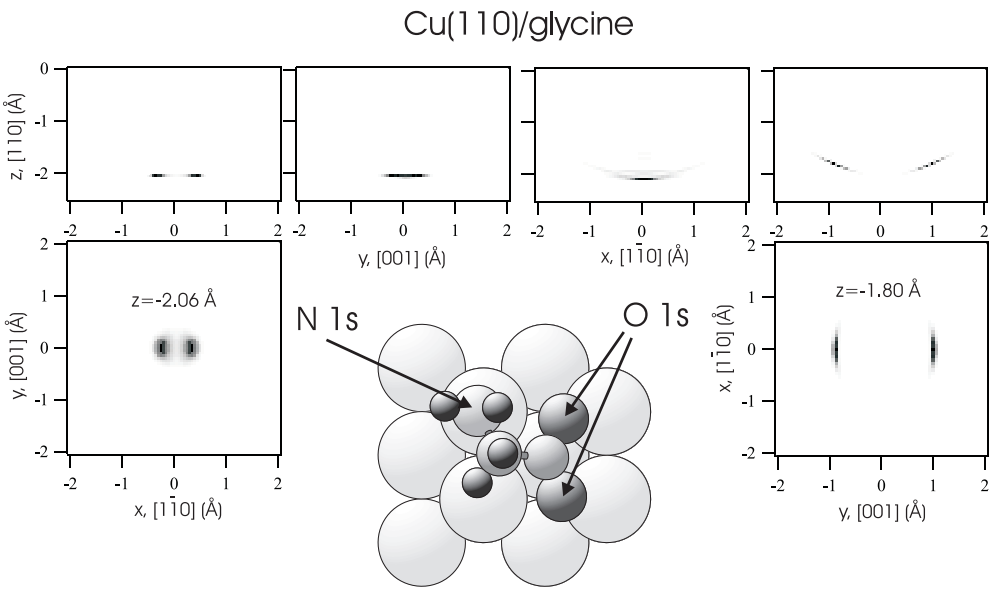

Figure 5. Projection method results from the N (left) and O (right) emitters in glycine adsorbed on Cu(110) [37]. Also shown is a plan view of the local adsorption structure obtained in this system. Note that the N is slightly off atop along ⟨110⟩ and leads to a splitting of the 'image' of the Cu atom below due to the presence of two symmetry-equivalent domains. A similar effect is seen from the O emitter, but in this case the splitting (and offset from atop) is much larger and occurs in ⟨100⟩.

of the individual atomic emitters in the molecule will occupy low-symmetry sites. Two rather different situations can arise as a result of this. In one, the molecule bonds to the surface through the interaction of two or more atoms of different elemental species, which may nevertheless each have single well-defined sites. Examples in this category which we have studied are Cu(110)/CN [36] and Cu(110)/glycine [37], where the overall position of the molecule is reasonably symmetric, so although the C and N in CN, and the O and N in glycine (strictly, glycinate, $NH_2CH_2COO–$) are in low-symmetry (off-atop or off-bridge) sites, each such atom occupies only a single well-defined site (and its symmetry-equivalent sites in other domains). In both of these cases the projection method yielded helpful images clearly compatible with the local geometry from each emitter species (figure 5 shows the results for the glycine case).

The second situation arising from interatomic bond-length mismatches is associated with adsorbed molecules in which atoms of the same element may be involved in the surface bonding. Systems of this kind which we have studied are of hydrocarbons such as C_2H_2 and C_2H_4 in which the molecular axis is parallel to the surface and C_6H_6 in which the molecular plane is parallel to the surface. In the case of C_2H_2 on Ni(111) [12] and Cu(111) [38] we have a rather special case in which the C–C distance is increased by interaction with the substrate such that it appears to exactly match the separation of the two inequivalent hollow sites and the C atoms at the two ends of the molecule thus occupy these high-symmetry sites as discussed above. The case of benzene is intrinsically more troublesome, because even if the molecule occupies a high-symmetry site (as appears to be the case), all of the C atoms, which are the core-level emitters, are placed in low-symmetry sites, and the fact that no substrate has true sixfold symmetry means that the C atoms must occupy at least two inequivalent low-symmetry sites. An example of this situation is provided by benzene adsorption on Ni(111); in this system there is a switch of local adsorption site with changing coverage, so

we have data for two distinct local geometries [48]. In both structures the projection method indicates atop C sites. Inspection of the various actual (and possible) structural models shows that this is not too surprising. In all cases some (or exceptionally all) of the C atoms in the molecule are in off-atop sites, while the other C atoms are in off-bridge or off-hollow sites. The projection method is based on the idea that some directions will show dominant near-neighbour backscattering, but for low-symmetry sites there are many symmetry-equivalent domains over which the experiment averages, so an emission direction which corresponds to backscattering for one domain may not do so for several other domains. For off-atop local emitters, however, normal emission is reasonably close to this backscattering direction for *all* domains, so even a modest modulation amplitude will be preserved by the domain averaging. The apparent atop site derived from the projection method thus simply indicates that *some* of the C atoms are probably near atop—as is true for all high-symmetry adsorption geometries on this surface. A more exaggerated manifestation of this problem was found in a study of the Ni(110)/benzene system [40] in which the full structure determination showed that the local adsorption geometry is such as to place none of the C atoms particularly close to atop; in this case the projection method failed to identify any clear signature of a dominant near-neighbour backscatterer.

Applications of the method to C_2H_4 on Ni(111) (see above) and Cu(110) [41] both indicated essentially atop sites for the C emitters, although on the (110) surface there was some apparent splitting of the backscatterer image suggesting a possible off-atop location. In both cases full analysis did reveal off-atop locations, although the symmetry of the adsorption geometry found on the Ni(111) is significantly higher. The question of whether the projection method is able to distinguish a true atop or off-atop site is actually rather subtle. Clearly on a low-symmetry substrate there are few domains over which to average and thus more chance of seeing the off-atop geometry, as for the N atoms in NH_3 and glycine mentioned above (see also figure 5). The large number of domains and multiple off-atop sites clearly favours a smearing around the atop site. However, the size and angular density of the PhD data set used in the inversion may also be relevant as discussed in the next section.

For C_2H_4 on Pd(110) [42] the projection method failed to yield a meaningful image; this is in part due to the particularly low-symmetry adsorption geometry found for this system, but may also be related to the character of the Pd substrate scattering, as discussed below.

5. Problems and limitations

5.1. General comments and introduction

On the basis of these experiences using the projection method it is possible to try to draw some general conclusions. Although the method has worked very well in many cases, we have also identified some limitations, especially related to the problems of low-symmetry emitter sites, and also some cases where the method appears to have failed to give any meaningful information. These cases have been investigated more carefully to try to understand the origins of the problem. We believe that many of the problems and limitations that we identify will also be relevant to other methods of direct data inversion in photoelectron diffraction and probably, insofar as the underlying ideas of the inversion methodologies are similar, to LEED. We prefix these details, however, with a general comment on the different inversion methods and the extent to which there success can be claimed to have been proven. As mentioned earlier, *all* of the direct methods in low-energy electron scattering are intrinsically approximate in that they take no account of problems such as multiple scattering, arguing that the effects of this may ‘wash out’ if one uses the right inversion algorithm. As a general rule, however, coherent

interference effects can lead to very strong effects in certain circumstances. Testing an idea with a single model (a common practice in the past) cannot, therefore, establish the general applicability of the method. In applying our method to some 30 different experimental data sets, we have identified a few cases of major failure of the method. However, in comparing our experiences with those with other methods, we should recognize that none of them have been tested on as many specific problems, so our identification of problems may reflect a weakness of our method, but may also reflect the fact that we have tested it far more severely. In particular, our method appears to work well for almost all the 'simple' cases, and most other methods have only been tested with this type of problem.

We now consider some further specific issues which have arisen from our tests. The issues that we address are: experimental data-set sizes and sampling density; the role of different atomic scattering cross-sections; multiple scattering; compound surfaces and element identification.

5.2. Size and sampling density of experimental data sets

While our primary object here is not to compare the projection method with other (notably holographic inversion) methods, one issue which has been the subject of some debate is the size of the database used in the inversion process. As remarked in the introduction, early explorations with holographic inversion concentrated on single-energy wide-angle scans of the emitted photoelectrons. The inversions obtained from such data were very poor, but including data from several (of order 10) such single-energy 'holograms' over a reasonably wide energy range (a few hundred eV) has proved far more promising. Our projection method is based on a quite different sampling of the photoelectron k-space. We typically measure PhD modulation spectra over a photoelectron energy range of around 80–450 eV in small (2–3 eV) steps, but in only 10–15 different directions (sometimes less). The angular acceptance of the measurements is a few degrees, the polar angular separation of the spectra is about 10° and the measurements are usually made in only 2–3 principle azimuths separated by 30–60° or even (on fcc(110) surfaces) 90°. An obvious question is: what is the optimum, and minimum, sampling for a reliable structural inversion?

At least in the context of the projection method, there are probably two components to this question, one concerned with identifying a nearest-neighbour backscatterer, the other with the precision of its location. In principle, just one PhD modulation spectrum recorded in the appropriate backscattering direction is sufficient to generate an approximately correct location for the backscatterer, but of course we do not know this direction is advance. In essence, this is the basis for the rather small number of directions used in our applications of the method. The initial data collection strategy aims to concentrate on those angular ranges in which strong modulations can be found, and these are the key spectra for the inversion. We also know that this size of data set yields precise (and apparently accurate) structural determinations when combined with multiple-scattering simulations, so we do not wish to have to use a much larger data set as input for an approximate method to precede the full analysis. However, the precision with which a backscatterer can be located must also depend on the angular intervals of the PhD spectra inverted; as we have already remarked in the context of the Ni(100)/C clock-reconstructed surface, if measurements are only made in high-symmetry azimuths, backscatterers are unlikely to be identified as occupying sites in intermediate azimuths. Of course, if we are only trying to identify the *approximate* scatterer location, this imprecision may not be important, so it is not clear that a finer data set is really worthwhile, at least for this strategy. This has certainly been our perspective in dealing with the question of true atop versus off-atop adsorption sites; if the projection method tells us the

site is at least approximately atop, we can establish the true situation far more reliably through multiple-scattering simulations.

Despite these comments, we have recently been investigating the possible importance of difference sizes of data sets using model calculations, although we have come to appreciate, from comparisons with real experimental data sets which have been subsequently reproduced by multiple-scattering simulations, that subtle effects such as correlated vibrations can contribute significantly to the success of the projection method. The fact that correlations in the vibrations of the emitter and nearest-neighbour atoms suppress the importance of more distant scatterers is helpful in a technique aimed only at identifying the location of these nearest neighbours. Here we should mention one published attempt to address the question of the optimum k-space sampling, in terms of energies and angles, for several different inversion methods including the projection method using a single simulated model data set [43]. For the projection method, at least, the results are very strange and not at all compatible with our experience; a notable feature, however, is that these tests used energy sampling from 3 values to 45 values, all significantly less than in our experiments and largely inadequate for a method aimed at exploiting modulation frequencies as a function of energy.

5.3. The influence of different atomic scattering cross-sections

We have remarked in the previous section on problems encountered in two adsorbate systems involving Pd substrates. For CO adsorption on the Pd(111) surface there are two different ordered phases, a $(\sqrt{3} \times \sqrt{3})$R30° phase at 0.33 ML, and a c(4 × 2) phase at 0.5 ML. In the former case the CO molecules all occupy fcc hollow sites, while in the latter fcc and hcp hollows are occupied with equal probability. Applying the projection method to the data from the lower-coverage phase provided a clear identification of the correct adsorption site, but for the higher-coverage phase no meaningful image was obtained. This type of failure is also found for Pd(110)/C_2H_2, although in this case the individual C atoms are in low-symmetry sites. Apparently there is some problem with the Pd substrate which is more challenging for the projection method; when adsorption is in a single high-symmetry site, the method yields satisfactory results, but with mixed sites of low-symmetry sites it does not.

We attribute this problem to the very different angle and energy dependence of the Pd scattering cross-section relative to that of Cu and Ni, in particular (but also Si), for which we have found the method to be generality successful. To illustrate this problem and explore its generality and implications, some simple calculations have been performed on the scattering properties of a range of elements of interest in PhD experiments. Figure 6 summarizes these electron scattering factors for atoms in a section of the Periodic Table covering the transition metals, the simple metals Mg and Al, and the elemental semiconductors Si and Ge. The (complex) scattering factors can be expressed in the form $f \exp(\mathrm{i}\theta)$ and figures 6(a) and 6(b) show respectively the modulus f and the phase θ. In each case the value of the relevant parameter is shown by a colour on a map in scattering angle (0–180°) and in electron energy from 50–350 eV. Considering first the scattering factor amplitude, f, we note that for the first transition series ending with Cu and Ni there is a clear peak around 180° backscattering (seen as green in the maps) with no comparable scattering cross-section until one reaches the much more intense forward-scattering peak around 0°. These scattering cross-sections thus favour the dominance of 180° backscattering in the adsorbate PhD experimental geometry, and match the conditions which are assumed to occur in the principles of the projection method. This is, however, not true for the second and third transition series. For Pd, for example, the 180° backscattering cross-section peak is lost in the intermediate-energy range, and the scattering cross-section is higher at some intermediate backscattering angles. In the third transition row

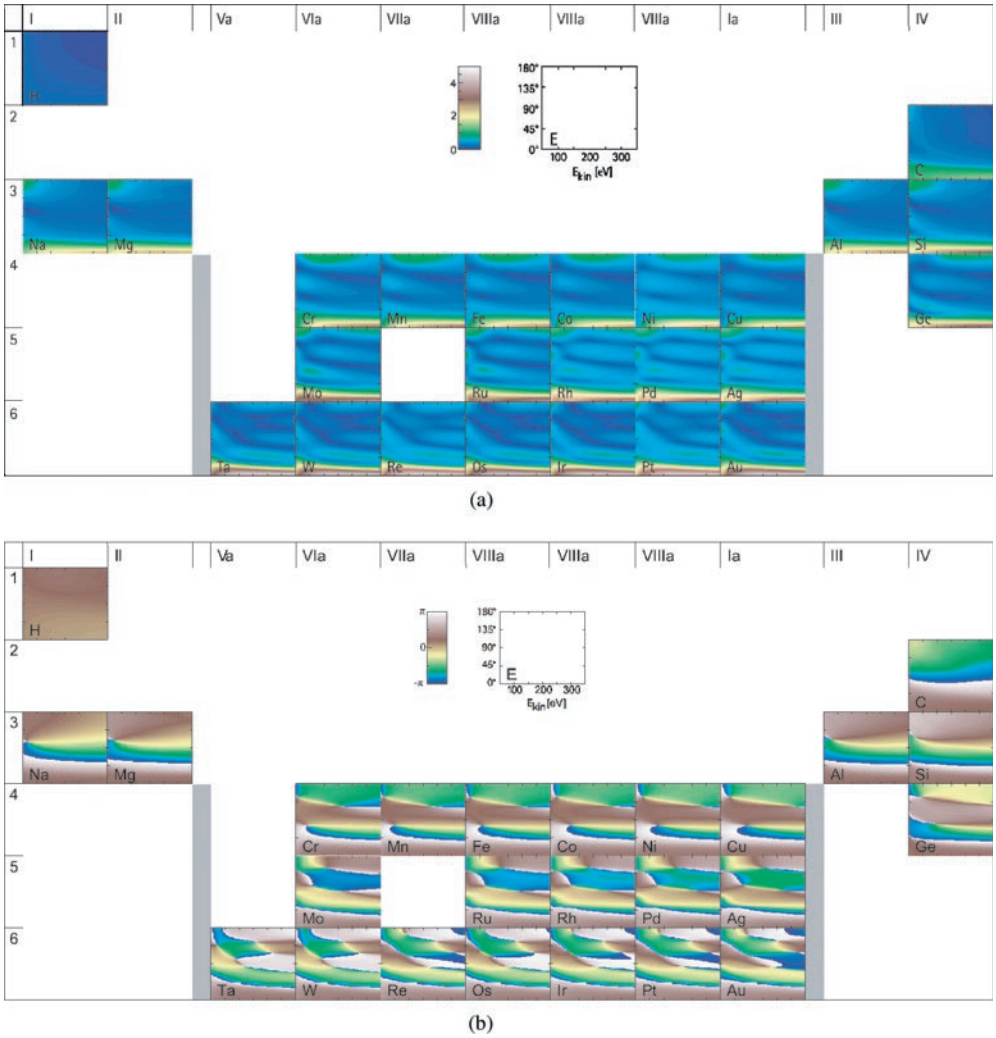

Figure 6. Electron scattering factor amplitude (a) and phase (b) for some of the elements as a function of scattering angle and kinetic energy (after [48]).

there is actually a low minimum in the 180° backscattering cross-section in the intermediate-energy range which is well known as a problem in EXAFS studies on Pt, for example.

A simple illustration of the potential impact of these differences in a PhD experiment is shown in figure 7, in which, arranged on the same Periodic Table grid, are the results of single-scattering calculations for a normal-emission scanned-energy-mode photoelectron diffraction modulation spectrum for an emitter atom on top of a single atom of the relevant species at a height of 2.0 Å (figure 7(a)) or placed at the same height over the hollow site created by four atoms of the relevant element on a square grid with a spacing of 5 Å (figure 7(b)). For an atop site on a cubic (100) surface with a nearest-neighbour distance of 2.5 Å these two models correspond to the role of scattering from the nearest-neighbour and to the four next-nearest-neighbour substrate atoms, respectively. Compare, now, the results for Ni and Pd. For the single substrate atom directly below the emitter the modulation spectra (figure 7(a))

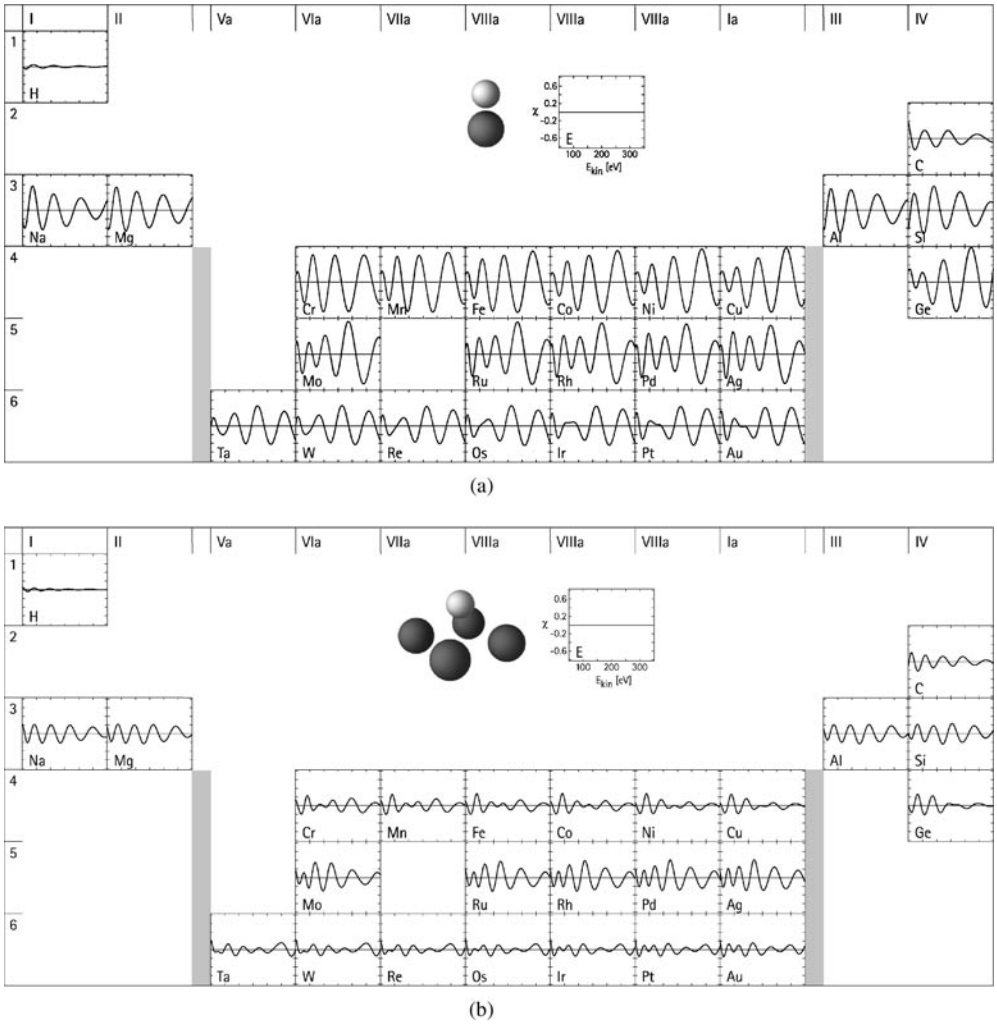

Figure 7. Single-scattering simulations of normal-emission PhD modulation spectra for different substrate scattering atoms for two different local scattering geometries: (a) emitter atop a single 'substrate' atom at a height of 2.0 Å and (b) emitter 2.0 Å above the centre of a square of four 'substrate' atoms separated by 5.0 Å (after [48]).

from these two elements are quite similar, although the phase of the modulations is opposite in most of the energy range, reflecting a difference in the two scattering phase factors (figure 6(b)) approximately equal to π. By contrast, the modulations arising from the four nearest neighbours shown in figure 7(b) are quite different; for Pd they are only about a factor of 2 weaker than for the nearest neighbour with 180° scattering angle, whereas for the Ni these modulations are a factor of several times weaker still. Clearly, the atoms in the first transition series present an especially favourable case for the projection method. By contrast, the second transition series is less favourable. We can then understand why when Pd is the substrate the method may still work satisfactorily for a single high-symmetry adsorption geometry, but yields poor results with multiple sites or low-symmetry emitters, despite the fact that these less favourable systems can be studied in many cases on Cu and Ni substrates.

Theses two figures also allow one to evaluate the situation for other elements. For Si, for example, the situation is still quite favourable, and indeed we have obtained satisfactory projection maps for the off-atop C emitters in the case of $Si(100)/C_2H_4$ [44]. The third transition series clearly is not without its problems for PhD in general, because of the weak scattering in the energy range around 100–200 eV, but the model calculations show that the contribution of the next-nearest neighbours may not be too severe in a direct data inversion. It is difficult to estimate the effect of these characteristic differences in the elastic scattering cross-sections on other methods of direct inversion of photoelectron diffraction data, but many of the same factors must come into play.

5.4. Multiple-scattering effects

A problem which has been widely recognized as potentially troublesome in any direct inversion of photoelectron diffraction (or holography) data is the role of multiple scattering. It is well established that effective simulations of experimental data in these techniques requires the inclusion of higher-order scattering, yet all of these methods effectively assume that single scattering dominates. Arguments have been presented as to why these methods may effectively suppress the importance of multiple scattering in the data inversions. We also know that in the special case of a substrate atom (at least of many elements) being in the favourable 180° backscattering geometry, a PhD spectrum is dominated by a single period which can be attributed to the scattering contribution from this single atom. Strictly, in this geometry double scattering, involving backscattering from the substrate atom and forward scattering from the emitter, also contributes to this spectrum, enhancing the intensity but slightly modifying the phase (and thus the apparent path-length difference), but this effect is not a major issue for the (approximate) structural image produced by the projection method. Recently, however, as remarked in the previous section, we have found two closely related systems in which the projection method has failed for relatively high-symmetry sites, and find that the origin of this failure appears to be the role of multiple scattering.

The two cases in which this problem has arisen are for the Cu(100)c(2 × 2)–N and Cu(100)($\sqrt{2} \times 2\sqrt{2}$)R45°–O systems. In both cases the adsorption site is close to a coplanar hollow site, although both involve a reconstruction which modifies this high-symmetry geometry slightly. In the case of Cu(100)($\sqrt{2} \times 2\sqrt{2}$)R45°–O [26] there is a missing-row reconstruction which means that one of the Cu nearest-neighbour atoms of the O emitter is missing, and the O atoms suffers a small lateral displacement from the original high-symmetry position. In the case of Cu(100)c(2 × 2)–N we have found an unusual outermost layer Cu rumpling [45, 46] which actually lowers the symmetry of the N site from fourfold to twofold symmetry, the two diagonal pairs of Cu nearest neighbours having slightly different heights above the underlying substrate. As far as we can tell from our simulations, these distortions do not contribute to the problem. Figure 8 shows the key results for the Cu(100)c(2 × 2)–N system, also including a schematic diagram of the local geometry. Application of the projection method using an experimental data set which includes PhD spectra out to 70° polar emission angle indicated that the nearest-neighbour Cu atoms were a few tenths of an ångström below the N emitter but in the ⟨110⟩ azimuth, whereas in the real structure they are in the ⟨100⟩ azimuth. This result is reproduced when the projection method is applied to the simulated (multiple-scattering) modulation spectra which gave the best fit to the experimental data, and it is these results which are shown in figure 8. Applying the same method of data inversion to spectra calculated omitting the role of higher-order scattering, however, yields projection maps which place these neighbours in the correct azimuthal directions, at a similar depth. In both cases the actual height differences between the N and Cu neighbours are too large by about 0.2 Å

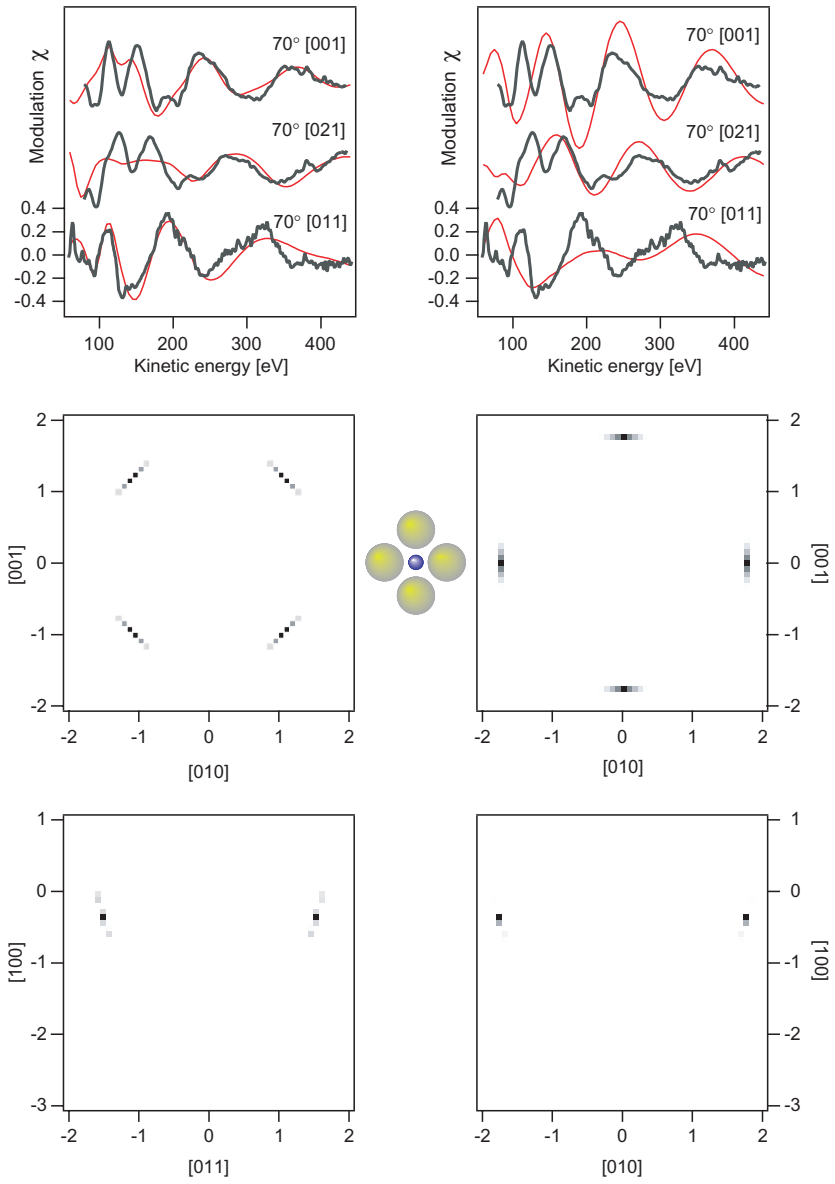

Figure 8. Results of applying the projection method to PhD data from the Cu(100)c(2 × 2)–N system. The results on the left are based on PhD spectra using multiple-scattering-theory simulations, while those on the right use similar calculations including only the single-scattering paths. The bottom panels show projection maps perpendicular to the surface in the azimuths cutting the highest-intensity features; note that these azimuths are different for the two data sets. The central panels show projection method maps parallel to the surface at depths below the emitter chosen to cut the dominant peaks in the bottom panel. Note that in the right-hand panel the peaks correspond to the correct positions of near-neighbour Cu atoms, but in the left-hand panels the structure is rotated by 45° and the emitter–scatterer distances are also shorter. The top panels show the actual PhD spectra at the largest polar angle used in the complete data set, and compare the experimental data with the results of the multiple-and single-scattering calculations. In the centre is a schematic plan view of the local structure showing the azimuthal directions of the four Cu nearest neighbours (larger spheres) in the outermost layer relative to the N emitter (small sphere).

but errors of this magnitude in directions perpendicular to the nearest-neighbour directions are not particularly disturbing. Placing the neighbours in the wrong azimuth, however, is far more surprising. Also shown in figure 8 are the PhD spectra associated with the largest polar emission angle (70°) which is closest to the ideal backscattering geometry for near-coplanar adsorption sites. Notice that in the experimental PhD spectra, it is the spectrum recorded in the [011] azimuth which appears to show the strongest single-period contribution, and it is this spectrum which is identified as the near-neighbour backscatterer direction by the projection method. However, the single-scattering simulation for this azimuth shows a much weaker modulation, of a different period, whereas the expected strong single modulation is seen in the true backscattering azimuth of [001]. Adding in the higher-order (notably double) scattering, however, reproduces the experimental spectra rather well; in particular, that recorded in the [011] azimuth now shows the single dominant period, whereas for emission in the [001] azimuth a splitting and attenuation of the single-scattering spectrum is obtained.

Although we have run test calculations for different component parts of the scattering cluster involved in this system, it is difficult to pinpoint the specific double-scattering events which cause this problem, but it appears to be associated with scattering events within the outermost surface layer, and so may well be a specific problem of near-coplanar adsorption sites. This one example (and very similar behaviour for the Cu(100/O structure) highlights, however, the general point that multiple scattering can achieve exaggerated importance in certain scattering geometries. Clearly, if these happen to be the geometries leading to the strongest PhD modulations, they will cause failures of the projection method, in particular, but quite possibly also of other inversion procedures. We should note, however, that in both of these cases the adsorbate emitter is only about 0.1 Å above the surrounding nearest-neighbour substrate scatterers, so strictly the data sets used in these structure determinations do not include measurements taken in the true 180° backscattering geometry, because the largest polar emission angle measured was 70° (which actually corresponds to this backscattering geometry for the emitter 0.6 Å above the nearest-neighbour Cu atoms). In the case of the Cu(100)($\sqrt{2} \times 2\sqrt{2}$)R45°–O phase, a projection method inversion was also performed on the experimental data set but with the addition of simulated spectra (using all the same parameters as those which matched the measured spectra) at a polar angle of 80°; the results in this case *were* compatible with the true structure. Very recently we have found that the same phenomenon occurs for Cu(100)c(2 × 2)–N. Strictly, therefore, these particular problems arising from the importance of multiple scattering correspond to cases in which the backscattering geometry is absent from the data set, and including these data overcomes the problem.

One important rider to this account of a clear failure of the method should be made. The positions of the nearest-neighbour Cu atoms implied by the incorrect projection maps are not compatible with known interatomic distances on a Cu(100) surface, and could only be interpreted as correct if there were a massive reconstruction of the surface. A radical restructuring of this kind would obviously be tested carefully by proper multiple-scattering simulations. The failure thus prevents the projection method from helping to solve the structure, but does not lead a reasonably careful practitioner to actually draw an incorrect conclusion concerning the true structure. These examples also highlight the need, however, to include PhD spectra which are reasonably close to the true backscattering direction to minimize the danger of failure of this kind.

5.5. Compound surfaces and the elemental identity of neighbours

One feature of the projection method, and (according to our understanding) all the holographic inversion methods, is that in order to correct for the effects of energy- and angle-dependent

scattering phase shifts, these properties of the scattering atoms are inserted into the computational procedure. This is perfectly satisfactory for an atomic adsorbate on an elemental substrate, but if the elemental identity of the neighbouring scattering atom is not known, this approach cannot be generally applied. In principle, this is a problem for intramolecular scattering in molecular adsorbates, but in practice the substrate atoms are usually the stronger scatterers (higher atomic numbers) and the data subjected to the inversion are chosen because they are most likely to be dominated by substrate scattering. On a compound surface, however, this is a fundamental problem. Although we are not aware of any proposed inversion scheme which addresses this problem, the fact that we have PhD data for several adsorbates (NO, CO, NH_3) on the (100) surface of NiO has led us to explore this problem, albeit not in great detail. In the case of a transition metal oxide, of course, the scattering cross-section of the O atoms is much smaller than of the transition metal atoms, so we might expect that distinguishing these neighbours should be rather straightforward. Indeed, through multiple-scattering simulations, this distinction is very clear, but finding a scheme of data inversion which is appropriately sensitive to this aspect is less clear. Our initial attempts to explore this problem have been described elsewhere [47], but in view of the lack of any clear positive conclusions we simply highlight here the existence of the fundamental problem.

6. General conclusions

The latter part of this paper, in particular, has concentrated on the problems identified in our applications of the projection method in direct inversion of PhD data for structure determination. Perhaps the first conclusion that we should draw from our experience, however, is how successful the method has proved, in general, in helping to identify the main ingredients of the local adsorption geometry. Nevertheless, it is the problems and limitations which are of greatest interest for the future of this and related methods. Our method may well be more limited in its aims than some of the holographic reconstruction methods, yet none of these methods can be expected to yield a complete and precise structure, and should never be regarded as a replacement for proper multiple-scattering analyses. Moreover, these other methods have been tested with very few experimental data sets, and almost all such tests (like those based on simulated data) have been based on high-symmetry adsorption structures. In this context many of our identified limitations are likely to be valid, to a greater or lesser extent, in these other methods.

Perhaps the most obvious general area of limitation is in the study of low-symmetry or multiple-site adsorption geometries. At least for molecular systems, these situations are very common, so this is not an extreme and atypical problem. The influence of averaging over symmetry-equivalent domains and multiple sites will inevitably weaken the influence of single sites or domains in the data, rendering inversion less effective, and even if the inversion does work correctly, the resulting 'images' are more complex and very probably show 'smeared' features.

Of the other problems which we have identified, some are generic and some may be specific to our method. For example, the problem of the strong influence of multiple scattering seen in the Cu(100)/N and Cu(100)/O systems (with adsorbates nearly coplanar with the outermost substrate atoms) may be largely attributable to the fact that the data sets used did not include emission angles sufficiently close to the ideal backscattering condition. This problem may be general only in highlighting the need for a sufficiently complete data set (though one should note that the smaller data set *was* sufficient for solving the structures by conventional modelling methods). The problem of the different 'signatures' of the energy and angle dependence of the scattering cross-sections of different elemental scatterers is probably

quite generic, if only because it influences the effective completeness of the scattering data set. Tackling compound surfaces and identifying the elemental character of scatterers in direct inversions is undoubtedly a very general problem. It may prove possible to address some of these problems in the future by using new and improved inversion algorithms, and by identifying the nature of the experimental data set which is optimum. Bearing in mind the need to complete any structure determination using photoelectron diffraction with some stages of 'trial-and-error' multiple-scattering simulations, however, it is important that any data set used for the direct inversion is also well suited to this second stage of surface structure determination.

Acknowledgments

This paper is heavily based on the results of studies carried out over a period of several years, and has thus had important input from many co-workers; these individuals are identified in the references cited here, but we specifically acknowledge their important role. We particularly acknowledge the important contributions of Philip Hofmann and Michael Schindler who first proposed the projection method, and Alex Bradshaw who directed the Berlin component of the Warwick–Berlin collaboration for many years. We also acknowledge the contribution of key funding, notably of the Physical Sciences and Engineering Research Council (UK) and the German Federal Ministry of Education, Science, Research and Technology (BMBF—contract number 05 SF8EBA 4).

References

[1] Hofmann P and Schindler K-M 1993 *Phys. Rev.* B **47** 13 941
[2] Hofmann P, Schindler K-M, Bao S, Bradshaw A M and Woodruff D P 1994 *Nature* **368** 131
[3] Woodruff D P and Bradshaw A M 1994 *Rep. Prog. Phys.* **57** 1029
[4] Woodruff D P, Davis R, Booth N A, Bradshaw A M, Hirschmugl C J, Schindler K-M, Schaff O, Fernandez V, Theobald A, Hofmann Ph and Fritzsche V 1996 *Surf. Sci.* **357/358** 19
[5] Watson P R, Van Hove M A and Hermann K 1999 *NIST Surface Structure Database Version 3.0* NIST Standard Reference Data Program, Gaithersburg, MD
[6] Barton J J 1988 *Phys. Rev. Lett.* **61** 1 356
[7] Dippel R, Woodruff D P, Hu X-M, Asensio M C, Robinson A W, Schindler K-M, Weiss K-U, Gardner P and Bradshaw A M 1992 *Phys. Rev. Lett.* **68** 1 543
[8] Fritzsche V and Woodruff D P 1992 *Phys. Rev.* B **46** 16 128
[9] Barton J J, Bahr C C, Hussain Z, Robey S W, Tobin J G, Klebanoff L E and Shirley D A 1983 *Phys. Rev. Lett.* **51** 272
[10] Schindler K-M, Hofmann Ph, Fritzsche V, Bao S, Kulkarni S, Bradshaw A M and Woodruff D.P 1993 *Phys. Rev. Lett.* **71** 2054
[11] Hofmann Ph, Schindler K-M, Fritzsche V, Bao S, Bradshaw A M andWoodruff D P 1994 *J. Vac. Sci. Technol.* A **12** 2045
[12] Bao S, Hofmann Ph, Schindler K-M, Fritzsche V, Bradshaw A M, Woodruff D P, Casado C and Asensio M C 1995 *Surf. Sci.* **323** 19
[13] Davila M E, Asensio M C, Woodruff D P, Schindler K-M, Schaff O, Weiss K-U, Fritzsche V and Bradshaw A M 1996 *Surf. Sci.* **359** 185
[14] Davila M E, Asensio M C, Woodruff D P, Schindler K-M, Hofmann Ph, Weiss K-U, Dippel R, Gardner P, Fritzsche V, Bradshaw A M, Conesa J C and González-Elipe A R 1994 *Surf. Sci.* **311** 337
[15] Hofmann Ph, Schindler K-M, Bao S, Fritzsche V, Ricken D E, Bradshaw A M and Woodruff D P 1994 *Surf. Sci.* **304** 74
[16] Theobald A, Schaff O, Hirschmugl C J, Fernandez V, Schindler K-M, Polcik M, Bradshaw A M and Woodruff D P 1999 *Phys. Rev.* B **59** 2313
[17] Schaff O, Hess G, Fritzsche V, Fernandez V, Schindler K-M, Theobald A, Hofmann Ph, Bradshaw A M, Davis R and Woodruff D P 1995 *Surf. Sci.* **331–333** 201

[18] Theobald A, Fernandez V, Schaff O, Hofmann Ph, Schindler K-M, Fritzsche V, Bradshaw A M and Woodruff D P 1998 *Phys. Rev.* B **58** 6768
[19] Fernandez V, Gießel T, Schaff O, Schindler K-M, Theobald A, Hirschmugl C J, Bao S, Bradshaw A M, Baddeley C, Lee A F, Lambert R M, Woodruff D P and Fritzsche V 1997 *Z. Phys. Chem.* **198** 73
[20] Gießel T, Schaff O, Hirschmugl C J, Fernandez V, Schindler K-M, Theobald A, Bao S, Berndt W, Bradshaw A M, Baddeley C, Lee A F, Lambert R M and Woodruff D P 1998 *Surf. Sci.* **406** 90
[21] Toomes R L, Lindsay R, Baumgärtel P, Terborg R, Hoeft J T, Koebbel A, Schaff O, Polcik M, Robinson J, Woodruff D P, Bradshaw A M and Lambert R M 2000 *J. Chem. Phys.* **112** 7591
[22] Bao S, Hofmann Ph, Schindler K-M, Fritzsche V, Bradshaw A M, Woodruff D P, Casado C and Asensio M C 1994 *J. Phys.: Condens. Matter* **6** L93
[23] Lindsay R, Theobald A, Gießel T, Schaff O, Bradshaw A M, Booth N A and Woodruff D P 1998 *Surf. Sci.* **405** L566
[24] Toomes R, Theobald A, Lindsay R, Gießel T, Schaff O, Didszuhn R, Woodruff D P, Bradshaw A M and Fritzsche V 1996 *J. Phys.: Condens. Matter* **8** 10 231
[25] Terborg R, Hoeft J T, Polcik M, Lindsay R, Schaff O, Bradshaw A M, Toomes R L, Booth N A, Woodruff D P, Rotenberg E and Denlinger J 2000 *Surf. Sci.* **446** 301
[26] Kittel M, Polcik M, Terborg R, Hoeft J T, Baumgärtel P, Bradshaw A M, Toomes R L, Kang J-H, Woodruff D P, Pascal M, Lamont C L A and Rotenberg E 2001 *Surf. Sci.* **470** 311
[27] Theobald A, Bao S, Fernandez V, Schindler K-M, Schaff O, Fritzsche V, Bradshaw A M, Booth N A and Woodruff D P 1997 *Surf. Sci.* **385** 107
[28] Hirschmugl C J, Schindler K-M, Schaff O, Fernandez V, Theobald A, Hofmann Ph, Bradshaw A M, Davis R, Booth N A, Woodruff D P and Fritzsche V 1996 *Surf. Sci.* **352–354** 232
[29] Hofmann Ph, Schindler K-M, Bao S, Fritzsche V, Bradshaw A M and Woodruff D P 1995 *Surf. Sci.* **337** 169
[30] Kang J-H, Toomes R L, Robinson J, Woodruff D P, Terborg R, Polcik M, Hoeft J T, Baumgärtel P and Bradshaw A M 2001 *J. Phys. Chem.* B **105** 3701
[31] Baumgärtel P, Lindsay R, Gießel T, Schaff O, Bradshaw A M and Woodruff D P 2000 *J. Phys. Chem.* B **104** 3044
[32] Booth N A, Davis R, Toomes R, Woodruff D P, Hirschmugl C J, Schindler K-M, Schaff O, Fernandez V, Theobald A, Hofmann Ph, Lindsay R, Gießel T and Bradshaw A M 1997 *Surf. Sci.* **387** 152
[33] Gießel T, Schaff O, Lindsay R, Terborg R, Baumgärtel P, Hoeft J T, Polcik M, Bradshaw A M, Koebbel A, Lloyd D R and Woodruff D P 1999 *J. Chem. Phys.* **110** 9666
[34] Terborg R, Polcik M, Hoeft J T, Kittel M, Pascal M, Kang J-H, Lamont C L A, Bradshaw A M and Woodruff D P 2000 *Surf. Sci.* **457** 1
[35] Franco N, Chrost J, Avila J, Asensio M C, Muller C, Dudzik E, Patchett A J, McGovern I T, Gießel T, Lindsay R, Fritzsche V, Bradshaw A M and Woodruff D P 1998 *Appl. Surf. Sci.* **123** 219
[36] Booth N A, Davis R, Woodruff D P, Crysostomou D, McCabe T, Lloyd D R, Schaff O, Fernandez V, Bao S, Schindler K-M, Lindsay R, Hoeft J T, Terborg R, Baumgärtel P and Bradshaw A M 1998 *Surf. Sci.* **416** 448
[37] Booth N A, Woodruff D P, Schaff O, Gießel T, Lindsay R, Baumgärtel P and Bradshaw A M 1998 *Surf. Sci.* **397** 258
[38] Bao S, Schindler K M, Hofmann Ph, Fritzsche V, Bradshaw A M and Woodruff D P 1993 *Surf. Sci.* **291** 295
[39] Schaff O, Fernandez V, Hofmann Ph, Schindler K-M, Theobald A, Fritzsche V, Bradshaw A M, Davis R and Woodruff D P 1996 *Surf. Sci.* **348** 89
[40] Kang J-H, Toomes R L, Robinson J, Woodruff D P, Schaff O, Terborg R, Lindsay R, Baumgärtel P and Bradshaw A M 2000 *Surf. Sci.* **448** 23
[41] Schaff O, Stampfl A P J, Hofmann Ph, Bao S, Schindler K-M, Bradshaw A M, Davis R, Woodruff D P and Fritzsche V 1995 *Surf. Sci.* **343** 201
[42] Baddeley C J, Lee A F, Lambert R M, Gießel T, Schaff O, Fernandez V, Schindler K-M, Theobald A, Hirschmugl C J, Lindsay R, Bradshaw A M and Woodruff D P 1998 *Surf. Sci.* **400** 166
[43] Len P M, Zhang F, Thevuthasen S, Kaduwela A P, Fadley C S and Van Hove M A 1997 *J. Electron. Spectrosc. Relat. Phenom.* **85** 145
[44] Baumgärtel P, Lindsay R, Schaff O, Gießel T, Terborg R, Hoeft J T, Polcik M, Bradshaw A M, Carbone M, Piancastelli M N, Zanoni R, Toomes R L and Woodruff D P 1999 *New. J. Phys.* **1** 20.1
[45] Driver S M, Hoeft J T, Polcik M, Kittel M, Terborg R, Toomes R L, Kang J H and Woodruff D P 2001 *J. Phys.: Condens. Matter* **13** L601
[46] Hoeft J T, Polcik M, Kittel M, Terborg R, Toomes R L, Kang J-H and Woodruff D P 2001 *Surf. Sci.* submitted
[47] Polcik M, Lindsay R, Baumgärtel P, Terborg R, Schaff O, Bradshaw A M, Toomes R L and Woodruff D P 1999 *Faraday Discuss.* **114** 141
[48] Baumgärtel P 2000 *PhD Thesis* TU Berlin (http://edocs. tu-berlin. de/diss/2000/baumgaertel_peter. htm)